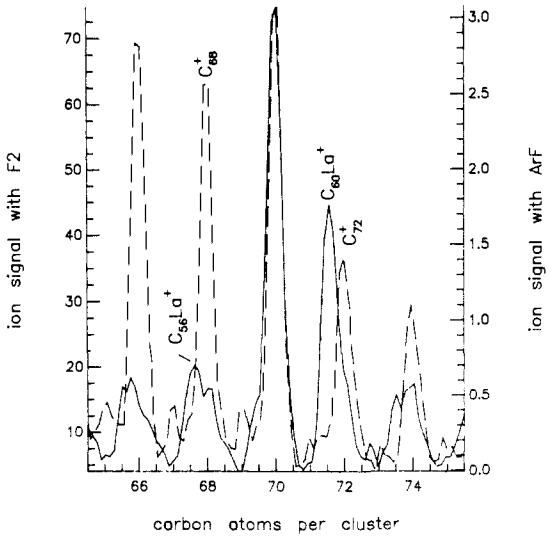

Figure 2. Expanded view of Figure 1 for the mass region spanning clusters containing 66–74 carbon atoms. The solid line and right-hand ordinate refer to the spectrum taken with ArF ionization and the dashed line and left-hand ordinate refer to the spectrum taken with F_2 ionization.

1a all the peaks are bare C_n. The C_nLa^+ ions are still present in Figure 1a but only appear as weak shoulders on the low-mass side of the bare cluster ions. This is more readily evident in Figure 2, which compares an expanded section of the two spectra presented in Figure 1. For quantitative comparison, these spectra are normalized to photon flux, which is reflected in the ordinate values. For these spectra we find that the photoionization efficiency for producing $C_{60}La^+$ is only 2–4 times larger with 7.87 eV than it is with 6.42 eV. On the other hand, the photoionization efficiency for producing the bare cluster ions, e.g., C_{60}^+, shows a dramatic increase of a factor of 50–100 with 7.87 eV compared to that with 6.42 eV.

Such dramatic changes in ion yields are due to the differing photophysical processes producing C_nLa^+ and C_n^+ during the ionization process. Both C_nLa^+ and C_n^+ ion signals vary linearly with F_2 ionizing laser intensity[5] at low intensity. Thus the spectrum obtained with F_2 should more closely approximate the actual neutral cluster concentration in the beam. With ionization at 7.87 eV the $C_{60}La^+$ signal is only 1–2% of the C_{60}^+ signal. If the $C_{60}La_2^+$ signal is also only 1–2% of the $C_{60}La^+$ as is reasonable in a sequential reaction, then observation of no signal on $C_{60}La_2^+$ for either ArF or F_2 ionization is *not* unexpected. $C_{60}La_2^+$ is simply produced in so small abundance as to be undetectable.[7] This together with the observation of a large number of C_nLa complexes may be more suggestive that the La atom is attached to the edge or face of graphite flakes rather than residing at the center of a spheroidal shell as proposed by HOLCKTS.

Finally, with ArF ionization a large "blob" of low-mass fragment ions is produced. The sharp peaks are assigned to La^+, LaC_2^+, $LaCl^+$, $LaCl_2^+$, LaC_4^+, $La_2Cl_5^+$, etc. The peak signal for these ions occurs *later* in time than the peak signal for the heavier mass C_nLa^+ which strongly suggests that they are fragments from very large clusters, C_nLa, $n \gg 60$. The total ion signal in this low-mass region is considerably larger than the C_{60}^+ or $C_{60}La^+$ signals when the ion signals are summed over all arrival times and corrected for transmission efficiency. These low-mass ions are produced when ionizing with ArF (0.4–1.8 mJ/pulse) or KrF[8] (5.0 eV, 1–2 mJ/pulse) but are absent when F_2 ($\leq$0.05 mJ/pulse) is the ionizing laser. Since the free La atom has an IP of 5.61 eV, it should be single-photon ionized by either 6.42- or 7.87-eV photons. Its appearance, as well as the appearance of all the low-mass ions containing La, in the 6.42-eV PMS but absence in the F_2 one strongly supports the contention that (a) substantial fragmentation is being induced by the higher intensity ArF[4] and (b) the lanthanum is complexed to carbon clusters.

In conclusion we show that under a specific set of experimental conditions certain ions may appear incredibly intense, whereas under a slightly different set of conditions these same ions may appear only weakly and/or other ions become quite intense.[9] Attempting to infer structural or stability information about neutral clusters simply from an intense (or weak) ion signal in a PMS is frought with complications which can lead one astray. However, the search for ultrastable structures, such as $C_{60}La$, i.e., a reinflated soccer ball, should not be abandoned, but rather a high priority should be put on developing techniques to perform direct structural characterization of such species.

(5) In our earlier work[6] we found that carbon clusters containing 40–80 atoms exhibited a linear dependence on ArF and KrF ionizing laser intensity. At that time we interpreted such behavior to mean that the ionization threshold for direct ionization was lower than 6.42 and 5 eV. Under the experimental conditions of those experiments (short extender length 1.27 cm and high vaporizing laser intensity 300–400 MW/cm^2), we were most likely dealing with internally hot clusters[9] undergoing substantial fragmentation during the ionization process.

(6) Rohlfing, E. A.; Cox, D. M.; Kaldor, A. *J. Chem. Phys.* **1984**, *81*, 3322–3330.

(7) When potassium-containing graphite rods are vaporized, clusters of the form C_nK, C_nK_2, and C_nK_3 are easily observed in the PMS.

(8) With ionization by KrF the C_n^+, and C_{60}^+, in particular, are quite weak compared to ArF whereas the signal level of the low-mass "blob" is nearly the same.

(9) We have observed similar behavior in our studies of silicon clusters, also molecular clusters. Trevor, D. J.; Cox, D. M.; Reichmann, K. C.; Kaldor, A., submitted for publication in *J. Chem. Phys.*

Electrochemical Preparation of Triplatinum Complex with a Linear Structure and Its Transformation to an A-Frame Structure

Yasuhiro Yamamoto,* Katsuo Takahashi, and Hiroshi Yamazaki

RIKEN (The Institute of Physical and Chemical Research), Wako, Saitama 351-01, Japan

Received January 13, 1986

The complexes containing metal–metal bonds have been the subject of reactivity and physical characterization. A-frame complexes have also been increasing attention on systematic cooperative binding and activation of substrates.[1] Recently Hoffman and Hoffmann employed the isolobal analogy between CH_2 d^{10} ML_2 and d^8 ML_4 metal fragments to predict the existence of a trimetallic cluster with one long and two short M–M bonds, a so-called "A-frame" with bridging ML_2 moiety.[2] To date, no complexes have been obtained.

Here we report a new aspect of the chemistry that led to the preparation and structure of linear and A-frame triplatinum complexes. The potentiostatic electrolysis of $[Pt(2,6\text{-}Me_2C_6H_3NC)_4](PF_6)_2$ (**1**) in CH_3CN containing 0.1 M $NaClO_4$ was carried out by means of a mercury pool electrode at −1.40 V.[3] The electrolysis consumed ca. 1.5 F and gave pale yellow and yellow crystals, formulated as $[Pt_2(2,6\text{-}Me_2C_6H_3NC)_6](PF_6)_2 \cdot CH_2Cl_2$ (**2**) (14%)[4] and $[Pt_3(2,6\text{-}Me_2C_6H_3NC)_8](PF_6)_2$ (**3**) (47%),[5] respectively. Complex **2** was assigned as a dimer by its

(1) Balch, A. L. *Homogeneous Catalysis with Metal Phosphine Complex*; Pignolet, L. H., Ed.; Plenum Press: New York, 1983; p 167. Puddephatt, R. J. *Chem. Soc. Rev.* **1983**, *12*, 99.

(2) Hoffman, D. M.; Hoffmann, R. *Inorg. Chem.* **1981**, *20*, 3543.

(3) The potentials are indicated against a saturated calomel electrode (SCE), although a $Ag/AgNO_3$-TBAP-CH_3CN electrode was employed.

(4) Anal. Calcd for $C_{55}H_{56}N_6P_2F_{12}Cl_2Pt_2$: C, 42.56; H, 3.64; N, 5.41. Found: C, 42.87; H, 3.61; N, 5.44. ^1H NMR (CD_2Cl_2): δ 2.56 (2,6-Me), 5.31 (CH_2Cl_2), ca. 7.2 (Ar H).

(5) ^1H NMR (CD_2Cl_2): δ 2.27 (2, 2,6-Me), 2.47 (1, 2,6-Me), ca. 7.2 (Ar H). Anal. Calcd for $C_{72}H_{72}N_8P_2F_{12}Pt_3$: C, 44.93; H, 3.77, N, 5.82. Found: C, 45.42, H, 3.81; N, 5.93.

0002-7863/86/1508-2458$01.50/0

Scheme I. Transformation of a Linear Structure to an A-Frame Structure[a]

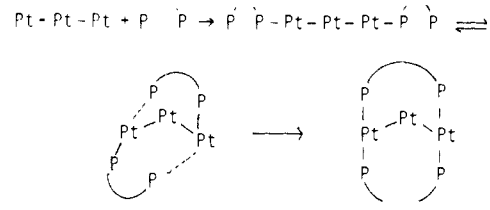

[a] Isocyanide ligands were omitted for clarity.

spectroscopic data. The infrared spectrum of **3** showed the presence of only terminal isocyanide ligands (2163 and 2149 cm^{-1}).

Reaction of **3** with PPh_3 produced a disubstitution product, $[Pt_3(2,6\text{-}Me_2C_6H_3NC)_6(PPh_3)_2](PF_6)_2\cdot CH_2Cl_2$ (**4**),[6] still showing the presence of only terminal isocyanide ligands in the infrared spectrum (2144 and 2126 cm^{-1}). The proton NMR spectra of **3** and **4** showed the presence of three and two kinds of *O*-methyl groups, respectively. In order to obtain an accurate structure, an X-ray structural investigation of **4** was undertaken.[7,8] The structure of the cation is illustrated in Figure 1. Three Pt atoms are collinear with the P atoms. Each Pt atom exhibits approximate square-planar geometry. The square planes are twisted away from each other and the angle between the two five-atom least-square planes is 81°, less twisted than that (74.5°) of the known $[Pd_3(MeNC)_6(PPh_3)_2](PF_6)_2$ complex.[9] The Pt–Pt bond length of 2.6389 (7) Å is longer by 0.05 Å than that of $Pt_2Cl_2(2,4\text{-}t\text{-}Bu_2\text{-}6\text{-}MeC_6H_2NC)_4$ (**5**).[10]

Addition of bis(diphenylphosphino)methane (dppm) to **3** gave yellow crystals formulated as $[Pt_3(dppm)_2(2,6\text{-}Me_2C_6H_3NC)_4](PF_6)_2\cdot CH_2Cl_2$ (**6**) (79%).[11] The infrared spectrum showed three peaks at 2174, 2118, and 2104 cm^{-1}, assignable to terminal isocyanide ligands. The proton NMR spectrum indicated two singlets at δ 1.66 and 2.03 in a 1:1 ratio, due to *O*-methyl groups, and a complicated resonances at δ ca. 4.5, due to methylene protons. The structure was determined by an X-ray analysis.[8,12] The molecular structure is given in Figure 2. The molecular geometry is a discrete A-frame structure. The geometries around platinum atoms are planar. The P ligands are bent away from the isocyanide ligands, giving rise to the mean value of 95° for the PPtC angle. The average Pt–Pt bond length is 2.593 Å, slightly shorter than those of **4**, $Pt_3(t\text{-}BuNC)_6$[13] and $Hg[Pt_3(2,6\text{-}Me_2C_6H_3NC)_6]_2$.[14] The nonbonded Pt(1)···Pt(2) distance is 3.304 (2) Å, longer than those found in $[Pt_2Cl_2(\mu\text{-}CH_2)(dppm)_2]$ (3.16 Å)[1] and $[Pt_2(\mu\text{-}CNCH_3)(CH_3NC)^{2+}\text{-}(dppm)_2]^{2+}$ (3.215 Å).[15] The Pt(1)Pt(2)Pt(3) angle is 80°, narrower by ca. 20° than the MCM angles.[15] This arises from

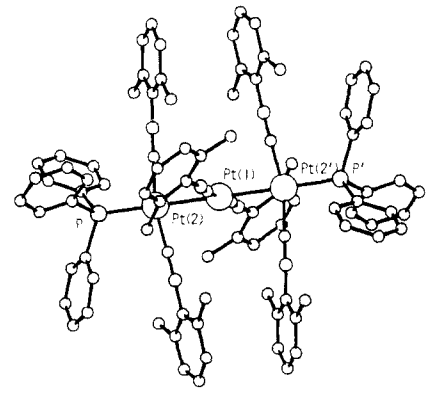

Figure 1. Molecular structure of $[Pt_3(2,6\text{-}Me_2C_6H_3NC)_6(PPh_3)_2]^{2+}$ (**4**).

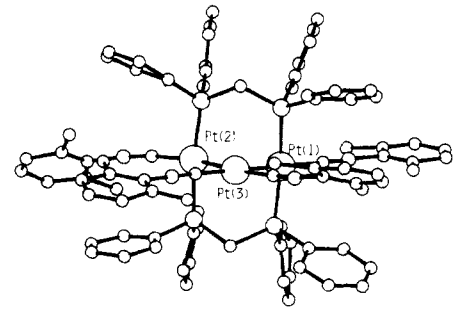

Figure 2. Molecular structure of $[Pt_3(2,6\text{-}Me_2C_6H_3NC)_4(dppm)_2]^{2+}$ (**6**).

difference of the bond radii of platinum and carbon atoms and also from difference in hybridization about the central platinum and carbon atoms. A similar reaction was observed in the reaction of $[Pd_3(2,6\text{-}Me_2C_6H_3NC)_8](PF_6)_2$[16] with dppm to give A-frame complex $[Pd_3(dppm)_2(2,6\text{-}Me_2C_6H_3NC)_4](PF_6)_2\cdot CH_2Cl_2$.[17]

In the transformation from **3** to **6**, we suggest that the initial substitution reactions of dppm to an axial isocyanide ligand occur as observed in the reaction of **3** with PPh_3. The PtPtPt bond is bent, and the A-frame structure would be completed by approach of other uncoordinated phosphorus site to a vacant axial position of a platinum atom in the γ-position and by elimination of an isocyanide ligand (Scheme I).

This complex can be regarded as the adduct generated by insertion of the 14-electron fragment $Pt(2,6\text{-}Me_2C_6H_3NC)_2$, being isolobal with CH_2, into the Pt–Pt bond of $[Pt_2(dppm)_2(2,6\text{-}Me_2C_6H_3)_2](PF_6)_2$ (**7**).[18] As expected, a reaction of **7** with $Hg[Pg_3(2,6\text{-}Me_2C_6H_3NC)_6]_2$, being a precursor of the 14-electron fragment, took place in toluene at reflux and gave **6** in a 73% yield.

This reaction is the first example of the A-frame structure formed by insertion of the 14-electron metal fragment into the metal–metal bond.

Synthesis and characterization of mixed-metal A-frame complexes by insertion of 14-electron species into $[M_2(dppm)_2\text{-}(RNC)_2](PF_6)_2$ (M = Pt, Pd) and related complexes are now in progress.

Supplementary Material Available: Tables of positional and thermal parameters of complexes **4** and **6** (4 pages). Ordering information is given on any current masthead page.

(6) ^1H NMR (CD_2Cl_2): δ 1.78 (2, 2,6-Me), 2.42 (1, 2,6-Me), 5.31 (CH_2Cl_2), 7.2 (Ar H). Anal. Calcd for $C_{91}H_{86}N_6P_4F_{12}Cl_2Pt_3$: C, 48.11; H, 3.82; N, 3.70. Found: C, 48.10; H, 3.75; N, 3.57.

(7) Crystal data: space group $P\bar{1}$, a = 13.979 (4) Å, b = 14.812 (6) Å, c = 11.872 (4) Å, α = 112.08 (3)°, β = 89.68 (3)°, γ = 97.27 (4)°, Z = 1, R = 0.065 using 4950 reflections having $F_o \geq 3\sigma(F_o)$.

(8) The full paper on the structural determination will be reported in the future.

(9) Balch, A. L.; Boehm, J. R.; Hope, H.; Olmstead, M. M. *J. Am. Chem. Soc.* **1976**, *98*, 7431.

(10) Yamamoto, Y.; Takahashi, K.; Yamazaki, H. *Chem. Lett.* **1985**, 201.

(11) Anal. Calcd for $C_{87}H_{82}N_4P_6Cl_2Pt_3$: C, 46.37; H, 3.67; N, 2.49. Found: C, 46.01; H, 3.60; N, 2.49.

(12) Crystal data: space group, $P2_12_12_1$, a = 21.861 (7) Å, b = 21.822 (8) Å, c = 18.146 (8) Å, β = 89.89 (3)°, Z = 4. R = 0.0852 using 4899 reflections having $F_o \geq 3\sigma(F_o)$.

(13) Green, M.; Howard, J. A.; Spencer, J. L.; Stone, G. A. *J. Chem. Soc., Chem. Commun.* **1975**, 3. Green, M.; Howard, J. A.; Murray, M.; Spencer, J. L.; Stone, F. G. A. *J. Chem. Soc., Dalton Trans.* **1977**, 1509.

(14) Yamamoto, Y.; Yamazaki, H.; Sakurai, T. *J. Am. Chem. Soc.* **1982**, *104*, 2329.

(15) Olmstead, M. M.; Hope, H.; Benner, L. S.; Balch, A. L. *J. Am. Chem. Soc.* **1977**, *99*, 5502.

(16) The complex was prepared according to the literature method.[9] Ir (Nujol): 2146, 2128, 2115 cm^{-1}. Anal. Calcd for $C_{72}H_{72}N_8P_2F_{12}Pd_3$: C, 52.14; H, 4.38; N, 6.76. Found: C, 52.66; H, 4.36; N, 6.76. In the ^1H NMR spectrum (CD_2Cl_2), *O*-methyl protons showed two peaks at δ 2.54 and 2.29 (broad and relatively sharp, respectively) in a 1:1 ratio. This suggests fluxionality between axial and central isocyanide ligands. The detail will be reported later.

(17) Ir (Nujol): 2146, 2128, 2115 cm^{-1}. Calcd for $C_{87}H_{82}N_4P_6F_{12}Cl_2Pd_3$: C, 52.57; H, 4.16; N, 2.82. Found: C, 52.44; H, 4.11; N, 2.68. The ^1H NMR spectrum in CD_2Cl_2 showed two singlets at δ 1.67 and 1.95 for *O*-methyl protons.

(18) This complex was prepared from **2** and dppm.